




Ultrasensitive light confinement: Driven by multiple bound states in the continuumHarsh K. Gandhi ¹, Arnab Laha ^{1,2} and Somnath Ghosh ^{1,*}¹*Unconventional Photonics Laboratory, Department of Physics, Indian Institute of Technology Jodhpur, Rajasthan-342037, India*²*Institute of Radiophysics and Electronics, University of Calcutta, Kolkata-700009, India*

(Received 10 March 2020; accepted 1 September 2020; published 30 September 2020)

We propose a framework to study the topological properties of an optical bound state in the continuum (BIC). Here, the formation of a BIC has been shown using the interaction between proximity resonances undergoing avoided resonance crossing in a simple fabrication, feasible gain-loss assisted microcavity. Similar to a Friedrich-Wingten (FW)-type BIC, the formation of an ultrahigh-quality (Q) mode due to the precise destructive interference between resonances has been reported. The enhancement in the Q factor was found to be more than four orders of magnitude greater than the other participating resonances. Furthermore, multiple such FW-type high- Q operating points from the same set of proximity resonances have been identified. Upon further inspection, we report the formation of a special-BIC line in the system parameter space connecting the locations of these operating points. Further, we closely investigate the light dynamics of systems near single and multiple quasi-BICs. Aiming to develop a scheme to enhance the performance of optical sensing in a microcavity, we study the sensitivity of transmission coefficients and quality factor to sense even ultrasensitive perturbations in the system configuration. Our proposed scheme would open up a vast potential for an enhanced desired optical response in enhanced nonlinear applications, low-threshold nano- and microlasers, and device-level sensors.

DOI: [10.1103/PhysRevA.102.033528](https://doi.org/10.1103/PhysRevA.102.033528)**I. INTRODUCTION**

The physics governing the interaction between resonances in optical platforms has become an ever-increasing area of research and development in the past few years. In particular, there has been an emphasis on the modeling of photonic systems such as optical microcavities towards a desired optical performance, which has been studied extensively [1]. Optical microcavities have the ability to confine light, enabling the formation of the high-energy density of light. This phenomenon is essential for various applications that are prevalent in the fields of nonlinear optics [2,3], biosensing [4], low-threshold lasing [5,6], and processing quantum informatics [7], to name a few. However, their performance is impaired by the task of identifying long-confined resonances with lower power requirements. Unlike bulk media [8,9], it is possible to enhance the Purcell factor by increasing the Q/V ratio, which is the effective quality factor (Q) of light over the modal volume (V) [10]. In this context, supercavity resonances have shown promise to accomplish the same [11–14]. Recently, an approach involving the interaction between two proximity resonances via the avoided resonance crossing (ARC) phenomenon was identified to hold great potential for the evolution of high- Q modes [15,16]. Furthermore, the application of the concept of ARC has been widely demonstrated in various resonator structures such as rectangular, semistadium, and elliptical microcavities [17].

In particular, the formation of one such high- Q state, i.e., the quasibound states in the continuum (BIC) [18,19], has

been extensively studied and reported. BICs are mathematical abstractions wherein a photonic BIC is a state that captures a high volume of energy, with theoretically infinite efficiency with closed radiation channels despite being in the continuum band [20,21]. In the case of a cavity, a BIC would have no leakage radiation outside the cavity and would theoretically confine light for an infinite time. However, a true BIC would require an infinite size of the cavity or an infinitely high permittivity of the medium [22,23], which is not physically implementable. Further, the practical feasibility of the realization of a BIC in various optical platforms is still an open area of research [24–26]. In this direction, it has been demonstrated that two cavity-supported resonances under a strong-coupling regime undergoing destructive interference could lead to one of them evolving with a higher Q [11–14,27]. This is in agreement with the Friedrich-Wingten (FW) theory of continuous parameter tuning [28]. The mechanism of such phenomenon originates from the precise destructive interference patterns [29] between the resonances that cancel out the losses from the radiation channel of the lossy modes. Thereafter, these states arise from the merger of multiple topological charges in the momentum space, thus attaining an impulsive growth in the Q factor [29]. The evolution of such finitely high- Q resonances is termed a *quasi-BIC state*.

In this paper, we report the formation of a FW-type quasi-BIC state between two longitudinal modes in a gain-loss (unbalanced) assisted optical resonator with enhancement in the Q factor up to four orders of magnitude. Devoid of any interference between Mie resonances, such Q enhancement has been obtained even for a choice of an overall lossy system (high loss and low gain). By exploiting the possibility of carefully tuning and optimizing the material gain-loss profile

*somiit@rediffmail.com

of the system, we sustain a quasi-BIC. Using ARC, we have shown that the enhancement in the quality factor is a consequence of the quasi-BIC state. Multiple sites of the merger of BIC-driven topological charges, as suggested in [29], have been identified to achieve multiple high- Q points of operation and exploit its topological nature of the structure to be able to perform with higher optical performance. Furthermore, we report the formation of multiple FW-type high- Q operating points arising from the same set of proximity resonances. These locations in the system parameter space were found to be connected by a straight line that we name the special-BIC line. This special-BIC line provides a new degree of freedom to explore further topological aspects of the BIC. Aiming to develop a scheme to enhance optical sensing in a microcavity, we show the ultrahigh sensitivity of the transmission coefficients and quality of the light state to be able to sense even slight perturbations.

II. DESIGN OF AN OPTICAL MICROCAVITY HOSTING A QUASI-BIC

In an ideal scenario, a resonance would exhibit a nearly infinite lifetime, in a case where the material loss is negligible. However, a practical scenario would contain material absorption losses that need to be dealt with. Physically realizable systems such as photonic dielectric resonators are open in nature. Therefore, the interaction and interference between proximity resonances could be extensively understood using non-Hermitian quantum mechanics. In this case, when we consider the interaction between two proximity resonances, the system could be expressed in terms of a second-order non-Hermitian Hamiltonian as

$$H = \begin{bmatrix} \eta_1 & 0 \\ 0 & \eta_2 \end{bmatrix} + \begin{bmatrix} 0 & V \\ W & 0 \end{bmatrix} = \begin{bmatrix} \eta_1 & V \\ W & \eta_2 \end{bmatrix}, \quad (1)$$

where $\eta_{1,2}$ are the complex passive states of the system, which are subjected to an external off-diagonal perturbation (V, W) similar to the system shown in [15,16]. However, in contrast to the model presented in [15], we employ an ARC analysis which takes into consideration the open nature of the system. The formation of the BIC using more than two proximity resonances would also follow a similar approach. However, we limit our discussion to exploring the features of a quasi-BIC from two proximity resonances. Here, we deliberately impose a condition of external coupling, $V \neq W^*$, to explain the formation of a quasi-BIC. Under this condition, the two states can now be coupled via the continuum. The formation of a quasi-BIC would then occur when one of these states attains a very high lifetime as a consequence of precise destructive interference.

Furthermore, under such a constraint, we can calculate the energy eigenvalues of the system as $E_{1,2} = (\eta_1 + \eta_2)/2 \pm \sqrt{[(\eta_1 - \eta_2)/2]^2 + VW}$. Here, we intentionally avoid the case of zero external perturbation ($VW = 0$) to avoid degenerate eigenvalues. Without any loss in generality, it is safe to say that on the basis of the value of VW , the states undergo ARC under different coupling regimes [30]. This ARC, thus established, generally induces mutual energy exchange, which in particular evolves with a longer-living state along with a subsequent decay in the lifetime of the latter [11,12].

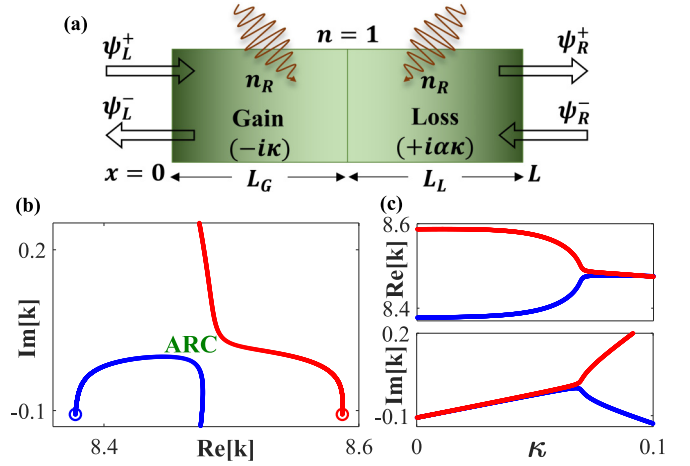


FIG. 1. (a) Schematic of the gain-loss assisted 1D Fabry-Pérot-type microcavity occupying the region $0 \leq x \leq L$. $\{\psi_L^+, \psi_L^-\}$ and $\{\psi_R^+, \psi_R^-\}$ represent the complex incident and scattered wave functions, respectively. (b) The dynamics of a pair of chosen coupled poles of the S matrix showing ARC in a complex k plane with an increasing κ for a fixed $\alpha = 2.23$. (c) The corresponding variation of the $\text{Re}[k]$ (upper panel) and $\text{Im}[k]$ (lower panel) with κ .

To implement this model, we design a two-port one-dimensional (1D) Fabry-Pérot-type optical microcavity, in which we carefully select a spatially varying gain-loss profile in a constant real background refractive index n_R , as can be seen in Fig. 1(a). However, the scheme involved can be extended to any resonator geometry. We place special emphasis on integrated photonic devices and hence, for this study, we restrict the value of the real refractive index $n_R = 1.5$ for silica-based glass. Note that there is no restriction on the selection of the geometry of the cavity, nor is there any constraint on the dimensions of the structure. We choose Fabry-Pérot-type resonators for the sake of understanding the interference physics between the participating longitudinal resonant modes along the axis of the cavity. Along the length of the resonator ($L = 10 \mu\text{m}$), we divide it into two sections having lengths L_G and L_L , which are the lengths of the material gain and material loss dominated regions. For the sake of simplicity, we take equal lengths for both sections, $L_L = L_G = 5 \mu\text{m}$. Along the length scale, the refractive indices profiles are defined as

$$\begin{aligned} n_G &= n_R - i\kappa, \\ n_L &= n_R + i\alpha\kappa, \end{aligned} \quad (2)$$

where n_G and n_L are, respectively, the complex refractive indices of the gain and loss regions. Here, κ is the gain coefficient and α is the ratio of loss-to-gain coefficients. The introduction of κ serves the purpose of introducing the system's non-Hermiticity. It also provides the ability to tune the system material for enhanced feasibility for fabrication. This tuning ability is per the causality condition of the Kramer-Konig relationship, which permits the flexibility of independent tuning of $\text{Im}[n]$ at a single frequency of operation [31,32].

To further study our system, we adopt the scattering matrix (S -matrix) formalism to numerically predict the behavior of the resonances. The elements of the S matrix can be

calculated using the analytical deduction from the electromagnetic scattering theory. Note that the system mentioned above is mathematically realized, but for the sake of physical implementation, we exploit the correlation between the poles of the S matrix and the eigenvalues of the Hamiltonian. This physical equivalence has been exploited to a great extent in the context of nonlinear dynamics of the system in Ref. [14]. A further selection of the virtual states represented by Eq. (1) is made by calculating the poles of the S matrix, which is of the form of

$$\begin{bmatrix} B \\ C \end{bmatrix} = S(n(x), \omega) \begin{bmatrix} A \\ D \end{bmatrix}, \quad (3)$$

where the incident and the scattered complex wave functions are represented by ψ_L^+ , ψ_R^- and ψ_L^- , ψ_R^+ , respectively, whose corresponding complex amplitudes are A , D and B , C , respectively. This calculation of the poles of the S matrix is numerically executed with the help of the numerical root finding method from

$$\frac{1}{\max[\text{Eig}(S)]} = 0, \quad (4)$$

where $\max[\text{Eig}(S)]$ are the maximal-modulus eigenvalues of the S matrix. In this model, we only calculate the poles of the S matrix in the fourth quadrant of the complex frequency plane (k -plane), in accordance with the current conservation and causality condition as well as for its physical feasibility [16,33]. As mentioned above, the entire analysis revolves around the fact that the obtained poles are indicative of the scattering states that are present inside the cavity. These proximity resonances contain the information related to the continuous confinement of the particle responsible for the scattering of the light and hence are justified to be equivalent to the poles of the S matrix in the k plane. For a given complex pole in the k plane, the imaginary part would depict the coupling loss that the pole undergoes during ARC. Here, it becomes vital to state that the coupling loss, which is the channel for radiation of the quasi-BIC, must be limited to null values for it to exhibit a diverging lifetime. The advent of the introduction of gain-loss within the system serves the purpose of reducing this coupling loss to theoretically zero values, manifesting nearly no leakage radiation from the quasi-BIC resonance.

We demonstrate the same, using two proximity resonances chosen in accordance with the structure dimensions as per [33]. We choose two proximity resonances between 8.3 and 8.7 μm in the $\text{Re}[k]$. With the introduction of gain-loss, these proximity resonances are mutually coupled in a specific coupling regime. It is noteworthy that the value of α in particular controls the coupling strength between the two participating states and governs the system openness. With a fixed parameter $\alpha = 2.23$, we increase the gain from 0 to 0.1. Upon this exercise, we observe the occurrence of an ARC phenomenon, with $\text{Re}[k]$ undergoing crossing and the $\text{Im}[k]$ having an anticross, as can be seen in Figs. 1(b) and 1(c). Upon close inspection, we observe the point of ARC in the system when the $\text{Re}[k]$ approaches 8.475 μm . The selection of parameters for α was on the basis of the observation of the divergence of the quality factor, which is defined as $0.5\text{Re}[k]/\text{Im}[k]$. Furthermore, we observe a divergence in Q

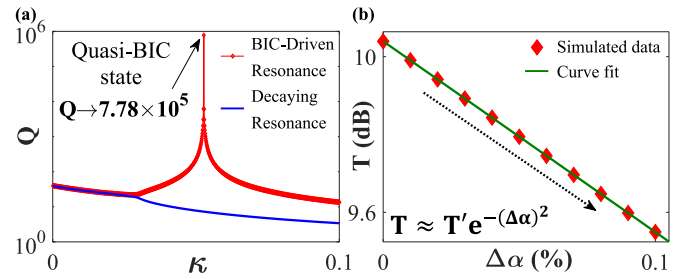


FIG. 2. (a) Q factor of the chosen coupled poles as a function of κ . Here, the divergence of the Q factor of a specific pole (represented by a red line with a diamond marker) has been observed near $\kappa = 0.0527$, which indicates the quasi-BIC state. The Q factor has been enhanced by more than four orders of magnitude greater than the decaying pole (represented by a blue line). (b) Transmission sensitivity due to the slight variation in α (in terms of $\Delta\alpha$) from the quasi-BIC state. The point at $\Delta\alpha = 0$ represents the transmission coefficient of the quasi-BIC state as indicated in (a), where the other points indicate different transmission coefficients for different $\Delta\alpha$.

of one of the resonances at a particular value of $\kappa = 0.0527$, where the Q diverges to more than four orders of magnitude, as can be seen in Fig. 2(a). In contrast, subsequent decay in the other resonance is also observed. We denote the Q factor of the pole at the quasi-BIC state as $Q_{\text{BIC}} \approx 7.78 \times 10^5$, while the subsequent decaying mode had a Q factor of $Q_{\text{decay}} \approx 7$. This simultaneous decay of one mode and the divergence of the other is of much importance for the understanding of why we call the latter a quasi-BIC. For the given carefully selected parameters of the system, we observe that one of the resonances decays in lifetime having characteristics similar to a continuum mode with very high leakage radiation, while the other, despite being in the same system preset, undergoes enhanced lifetime from a very low to ultrahigh Q factor.

Another aspect of our system is that it is overall lossy. We ensure this by taking the value of $\alpha > 1$. This is of physical significance, as natural materials that are considered for fabrication always possess absorption losses. However, even in cases of $\alpha \leq 1$, there is a possibility of a formation of a BIC. In this paper, we deliberately limit the study to overall lossy structures to study their capabilities to host high- Q resonances by virtue of quasi-BIC formation. Needless to say, in both cases, the amount of gain, which is lower than the amount of loss, or vice versa, has the role of inducing interference patterns that are out of phase and hence destructive in nature.

The extremely diverging values of Q that we obtain from a quasi-BIC driven resonance have their dependence on a variety of system parameters. In fact, the quasi-BIC could also be explored with the change in the length of both the gain and loss regions. However, in this paper, we limit our discussion by fixing our physical dimensions as constants so as to realize the effects of other critical system parameters, namely, the ones that govern the system absorption losses. In our system, these parameters are κ and α . For this purpose, to investigate the potential sensing abilities that these structures provide, we try to introduce an irregularity in the gain-loss profile. However, to carry this out in a systematic manner, we keep the material of the gain region intact and vary the material of the second block that is loss dominated. This can be done

with the introduction of small index modifications that can change the loss coefficient. We only introduce index change as low as 1% variation in α so as to test the sensitivity for small perturbations. In summary, we vary the α for a fixed gain, as can be seen in Fig. 2(b). We further study the transmission coefficients of the system at and around the quasi-BIC in the system parameter space. Here, in the case of $\Delta\alpha = 0$, we get transmission coefficients at the quasi-BIC state. Now we find the transmission of light through the structure for all different systems that we derive by changing α by 1% to 10% of the original $\alpha = 2.23$. By plotting them with the change in α in a logarithmic scale, and subsequently curve fitting them, we observe an inverse square dependence of loss-to-gain ratio on the transmission. We empirically find that transmission coefficients T follow an exponential decay, given by $\ln(T) \approx \ln(T') - (\Delta\alpha)^2$, where T' refers to the transmission coefficients of the system calculated at the quasi-BIC system configuration.

III. FORMATION OF A SPECIAL-BIC LINE TOWARDS ENHANCED SENSITIVITY

Utilizing the same proximity resonances, we work out different configurations of the system with constant length, where there is enhanced trapping of light. In this context, we confirm the claim with the help of ARC between the poles, now in the presence of different tunable parameters α and κ . For this analysis, we deliberately use structures that have properties of high absorption loss. For the corresponding values of α , we find a different κ , which is other than the κ for the quasi-BIC state we have reported earlier. We report five such high- Q operating points in the parameter (κ, α) plane that have similar properties as reported above. All of these points are sites of the merging up of multiple topological charges in the complex momentum space, inevitably leading to very high Q . As these active sites have properties similar to the quasi-BIC, we refer to them as multiple high- Q points driven by a quasi-BIC. Upon close inspection, we have discovered that all of these special points, identified and labeled as high- Q points driven by a quasi-BIC (using the similar process of ARC), lie on a straight line in the parameter (κ, α) plane. This straight line, which connects all the discrete high- Q points as depicted in Fig. 3(a), is referred to as a special-BIC line. A simple technique to check if any point is a quasi-BIC state in the parameter space is to check the ratio of the Q factor of the resonance that shows enhancement in the Q factor, at the configuration defined by the (κ, α) parameters to the Q factor of the same resonance supported by a passive cavity. The presence of a quasi-BIC state would be well established when the ratio, as mentioned above, would diverge to enormous values. Furthermore, we find that the high- Q point driven by the quasi-BIC at $\alpha = 2.23$ and $\kappa = 0.0527$, found earlier, lies on this special-BIC line, which we cross verify by extrapolating the special-BIC line. Interestingly, this line could be instrumental for understanding the BIC physics straightforwardly as the cumbersome task of identification and labeling of a high- Q point driven by various quasi-BIC states could be bypassed. Thus, the formation of such a BIC line introduces a new degree of freedom for the exploration of unconventional BIC physics in various cavity geometries.

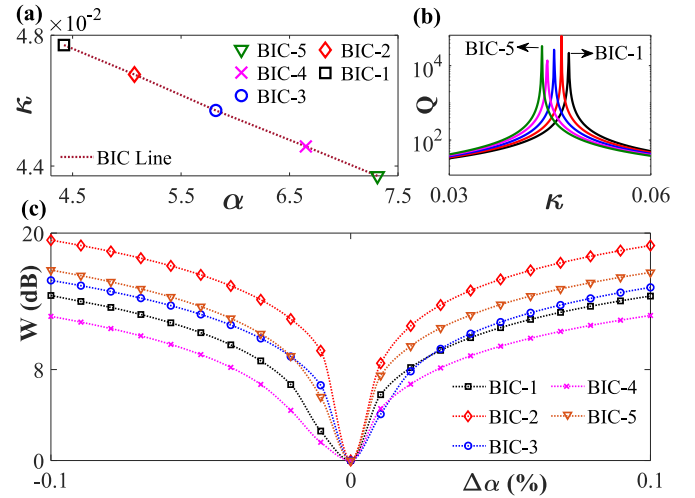


FIG. 3. (a) Multiple high- Q points driven by quasi-BIC states (indicated by the figure legend) between the same pair of coupled poles for different gain-loss pumping in the (κ, α) plane, which form a straight line (fitted), coined as the special-BIC line (indicated by the dotted brown line). (b) The verification of these five high- Q points driven by various quasi-BICs points of operation in terms of diverging Q factors. The different colors of the Q factors of five quasi-BICs correspond to the colors used to indicate the respective high- Q points driven by different quasi-BICs in (a). Here, the peaks (gradually, from right to left) represent the highest- Q factors of BIC-1 to BIC-5. (c) Sensitivity coefficients W with the variation of $\Delta\alpha$ due to a slight perturbation for all five high- Q points driven by multiple quasi-BICs. All of them show at least a 3.4 dB sensitivity response for a 1% change in the α .

For a more detailed study of these high- Q points driven by multiple quasi-BIC states, we study the isolated Q factors of the same resonances under the different quasi-BIC gain-loss configurations. The same has been plotted in Fig. 3(b), where the quality factor variation with κ has been color coded with the five high- Q points driven by a quasi-BIC, as can be seen in Fig. 3(b). We notice that the increase in α would require a lesser amount of κ to be introduced in the system. This inverse relationship between the parameters is of paramount importance from the fabrication point of view. With the help of state-of-the-art fabrication and implementation techniques, the scheme could be implemented with ease in different applications such as low-threshold lasers and integrated photonic devices [34] for higher optical performance.

Furthermore, in the direction of understanding the device application and the utility of the special-BIC line, we define a new parameter $W = -10 \log_{10}(Q/Q_0)$, where Q is the quality factor at a given set of parameters (κ, α) , and Q_0 is the Q factor at the high- Q points driven by a quasi-BIC. Here, we express W in decibels. This parameter W captures the change in quality factor due to the change in the parameters of the system. This is interesting in the sense of detecting any small perturbation inducing material changes in the system. These small perturbations that make changes in the system could, as a consequence, change this sensitivity coefficient W . Since Q is a quantity that is measurable with ease with modern advances and technological development, parameter W would unarguably be more physically realizable. Similar to

the transmission sensitivity study we have performed earlier, the sensitivity of the quality factor as we move away from the quasi-BIC driven high- Q point of operation has been studied. In this direction, we plot sensitivity in terms of the quality factor as opposed to sensitivity in terms of the transmission characteristics. The analysis has been performed by keeping the gain constant and varying the α parameter. We try to plot for all five high- Q points driven by a quasi-BIC that we obtain, and curve fit them for better visualization and extrapolation. A change of more than 12.7 dB in degree of confinement, for a 10% change in α , as compared to the configuration supporting quasi-BIC, was identified. In fact, the high- Q point driven by quasi-BIC-2 achieves a sensitivity factor of more than 20 dB with the same change. Upon much closer inspection, we find that the curve has a significant change with even smaller changes away from the BIC. The magnitude of the change for a smaller perturbation as small as 1% for high- Q points driven by quasi-BIC- i for $i = 1, 2, 3, 4, 5$ are as high as 9.6 dB for quasi-BIC-2. Please note that the nomenclature for naming the BICs is the same as expressed in the special-BIC line. Unlike transmission properties having an empirical dependence on the material properties, there seemed to be no distinctive concrete relationship between the quality factors of different high- Q points driven by different quasi-BICs. For illustration, high- Q points driven by quasi-BIC-2 have maximum sensitivity despite having lower κ values or lower gain in the system to close the radiation channel. Therefore, we can safely say that the gain in such a system that is governed by ARC would have the function of making sure that the leakage losses are being reduced to null, despite the fact that the system is lossy overall. We emphasize that these results could be implemented in different structures to enhance different optical performances; however, the underlying principle guiding the quasi-BIC would be similar.

IV. CONCLUSION

In summary, we exploit the phenomenon of ARC to enhance the degree of confinement of light in a Fabry-Pérot-type resonator equipped with varying gain and loss character. A drastic divergence of a lifetime up to four orders of magnitude as we approach the quasi-BIC state has been outlined. Notably, the ability to host a quasi-BIC through proper parameter tuning is utilized. This fine-tuning ability was then extended where distinct high- Q points driven by multiple quasi-BIC states led to the formation of a special-BIC line to provide a new degree of freedom to study the BIC physics in resonators. In addition, the study of a quasi-BIC driven system in the direction of developing a sensor capable of detecting ultrasmall perturbations has been reported. In this context, we closely inspect light dynamics at and around single and multiple quasi-BICs in terms of system transmission and divergence of the Q factor. These results, to optimize modes giving ultra-enhanced optical performance, open up a massive potential in terms of many applications such as biosensing and imaging, high-performance integrated photonic devices, low-threshold nano- and microlasers, and device-level sensors. We believe that these results, through state-of-the-art fabrication techniques and with more advancements in resonator physics, could open up further research and approaches in various fields of nonlinear optics and metamaterial physics.

ACKNOWLEDGMENTS

We acknowledge the financial support from the Science and Engineering Research Board (SERB) (Grant No. ECR/2017/000491) and the Ministry of Human Resource Development (MHRD), Government of India.

-
- [1] K. Vahala, *Nature (London)* **424**, 839 (2003).
 - [2] Z. Lin, X. Liang, M. Loncar, S. G. Johnson, and A. W. Rodriguez, *Optica* **3**, 233 (2016).
 - [3] L. Carletti, S. S. Kruk, A. A. Bogdanov, C. De Angelis, and Y. Kivshar, *Phys. Rev. Research* **1**, 023016 (2019).
 - [4] T. Yoshie, L. Tang, and S. Y. Su, *Sensors* **11**, 1972 (2011).
 - [5] W. Huang, Y.-H. Liu, K. Li, Y. Ye, D. Xiao, L. Chen, Z.-G. Zheng, and Y. J. Liu, *Opt. Express* **27**, 10022 (2019).
 - [6] B. Midya and V. V. Konotop, *Opt. Lett.* **43**, 607 (2018).
 - [7] T.-J. Wang, S.-Y. Song, and G. L. Long, *Phys. Rev. A* **85**, 062311 (2012).
 - [8] M. Soljacic, M. Ibanescu, S. G. Johnson, Y. Fink, and J. D. Joannopoulos, *Phys. Rev. E* **66**, 055601(R) (2002).
 - [9] P. Biswas, H. K. Gandhi, and S. Ghosh, *Opt. Lett.* **44**, 3022 (2019).
 - [10] K. Koshelev, S. Lepeshov, M. Liu, A. Bogdanov, and Y. Kivshar, *Phys. Rev. Lett.* **121**, 193903 (2018).
 - [11] A. A. Bogdanov, K. L. Koshelev, P. V. Kapitanova, M. V. Rybin, S. A. Gladyshev, Z. F. Sadrieva, K. B. Samusev, Y. S. Kivshar, and M. F. Limonov, *Adv. Photon.* **1**, 016001 (2019).
 - [12] M. V. Rybin, K. L. Koshelev, Z. F. Sadrieva, K. B. Samusev, A. A. Bogdanov, M. F. Limonov, and Y. S. Kivshar, *Phys. Rev. Lett.* **119**, 243901 (2017).
 - [13] M. Rybin and Y. Kivshar, *Nature (London)* **541**, 164 (2017).
 - [14] C. W. Hsu, B. Zhen, A. D. Stone, J. D. Joannopoulos, and M. Soljacic, *Nat. Rev. Mater.* **1**, 16048 (2016).
 - [15] H. K. Gandhi, D. Rocco, L. Carletti, and C. D. Angelis, *Opt. Express* **28**, 3009 (2020).
 - [16] A. Laha and S. Ghosh, *Opt. Lett.* **41**, 942 (2016).
 - [17] J. Wiersig, *Phys. Rev. Lett.* **97**, 253901 (2006).
 - [18] Q. H. Song, L. Ge, J. Wiersig, and H. Cao, *Phys. Rev. A* **88**, 023834 (2013).
 - [19] Q. H. Song and H. Cao, *Phys. Rev. Lett.* **105**, 053902 (2010).
 - [20] F. H. Stillinger and D. R. Herrick, *Phys. Rev. A* **11**, 446 (1975).
 - [21] K. Koshelev, A. Bogdanov, and Y. S. Kivshar, *Sci. Bull.* **64**, 836 (2019).
 - [22] C. W. Hsu, B. Zhen, J. Lee, S. L. Chua, S. G. Johnson, J. D. Joannopoulos, and M. Soljacic, *Nature (London)* **499**, 188 (2013).
 - [23] F. Monticone and A. Alu, *Phys. Rev. Lett.* **112**, 213903 (2014).
 - [24] D. C. Marinica, A. G. Borisov, and S. V. Shabanov, *Phys. Rev. Lett.* **100**, 183902 (2008).
 - [25] G. Ordonez, K. Na, and S. Kim, *Phys. Rev. A* **73**, 022113 (2006).

- [26] L. Carletti, K. Koshelev, C. De Angelis, and Y. Kivshar, *Phys. Rev. Lett.* **121**, 033903 (2018).
- [27] A. Cerjan, C. W. Hsu, and M. C. Rechtsman, *Phys. Rev. Lett.* **123**, 023902 (2019).
- [28] H. Friedrich and D. Wintgen, *Phys. Rev. A* **32**, 3231 (1985).
- [29] J. Jin, X. Yin, L. Ni, M. Soljacic, B. Zhen, and C. Peng, *Nature (London)* **574**, 501 (2019).
- [30] E. Teller, *J. Phys. Chem.* **41**, 109 (1937).
- [31] S. Phang, A. Vukovic, S. C. Creagh, T. M. Benson, P. D. Sewell, and G. Gradoni, *Opt. Express* **23**, 11493 (2015).
- [32] H. K. Gandhi, A. Laha, S. Dey, and S. Ghosh, *Opt. Lett.* **45**, 1439 (2020).
- [33] L. Ge, Y. D. Chong, S. Rotter, H. E. Türeci, and A. D. Stone, *Phys. Rev. A* **84**, 023820 (2011).
- [34] Z. Yu, X. Xi, J. Ma, H. K. Tsang, C-L. Zou, and X. Sun, *Optica* **6**, 1342 (2019).